



ELSEVIER

Contents lists available at [SciVerse ScienceDirect](http://www.sciencedirect.com)

Optics & Laser Technology

journal homepage: www.elsevier.com/locate/optlastec

Femtosecond laser ablation of indium tin-oxide narrow grooves for thin film solar cells

Qiumei Bian^{a,*}, Xiaoming Yu^a, Baozhen Zhao^b, Zenghu Chang^c, Shuting Lei^a

^a Industrial and Manufacturing Systems Engineering, Kansas State University, Manhattan, KS 66506, USA

^b Department of Physics, Kansas State University, Manhattan, KS 66506, USA

^c The Department of Physics and CREOL, University of Central Florida Orlando, FL 32816, USA

ARTICLE INFO

Article history:

Received 30 March 2012

Received in revised form

15 June 2012

Accepted 18 June 2012

Keywords:

Ablation

Femtosecond laser

Indium tin oxide

ABSTRACT

Finding ways to scribe indium-tin oxide (ITO) coating plays an important role in the fabrication and assembly of thin film solar cells. Using a femtosecond (fs) laser, we selectively removed the ITO thin films with thickness 120–160 nm on glass substrates. In particular, we studied the effect of laser pulse duration, laser fluence and laser scanning speed on the ablation of ITO. The single pulse ablation thresholds at various pulse durations were determined to ablate ITO thin films. Clean removal of the ITO layer was observed when the laser fluence was above the threshold of 0.30 J/cm². Furthermore, the morphologies and microstructure of fabricated grooves were characterized using a scanning electron microscope and KLA Tencor P-16 Profiler. A groove width down to 3 μm with 10 nm groove ridge can be achieved by the ablation of femtosecond laser pulses with 220 nj of energy. The femtosecond laser therefore provides a unique scheme to ablate the indium tin-oxide layer for the fabrication of thin film solar cells.

Published by Elsevier Ltd.

1. Introduction

Currently indium tin oxide (ITO) is widely employed as a transparent conductor for the fabrication of thin film solar cells [1,2]. The ITO layer in thin film solar cell modules has a significant impact on the power conversion efficiency [3,4]. In order to reduce the resistive losses and lost active area of solar cells, high resolution-patterning of ITO thin films is required in the formation of interconnect lines and assembly of thin film solar cells [5]. Various techniques have been developed to pattern ITO electrodes with well defined edges and electrically insulated grooves between the conductor lines for thin film solar cells. Examples include photolithography with wet etching in acidic solutions [6]. However, this method requires multiple process steps and expensive equipment as well as toxic chemicals. Also, the grooves with diffusion edges can be observed due to under or over etching. Therefore, it is necessary to develop a nonlithographic or direct patterning strategy to fabricate fine structures with well defined edges on ITO electrodes.

Laser ablation is the removal of materials from a substrate by direct absorption of laser energy, which can produce the desired combination of narrow and clean patterning because of their advantage in localized heating and material removal [7–9].

In general, ultrashort pulsed laser ablation offers small thermally induced defects in the remaining material, which are often difficult to avoid with longer laser pulses [10]. Therefore, femtosecond (fs) and picosecond (ps) lasers have been utilized to scribe ITO for the fabrication of solar cells [11–13]. Recent investigations on ps laser scribing of ITO demonstrated that the material damage threshold depends on laser repetition rate and wavelength, as well as other system parameters. It was also found that the groove edges were thermally affected by the use of 532 nm radiation, and the lowest ridge height of 20 nm was achieved [14]. Compared with ps laser pulses, fs laser can induce non-thermal structural changes driven by electronic excitation [7]. Femtosecond laser has been used as the precision material remove tool in solar cell fabrication research due to small thermally induced defects in the remaining material [15–17]. Ashkenasi et al. reported a theoretical and experimental investigation on fs laser ablation and concluded that a further improvement in quality can be obtained by using fs pulses in the IR spectrum [18]. Choi et al. [16] demonstrated fs laser ablation of ITO films with various pulse repetition rates and laser fluence. It was shown that the groove ridge is as high as 20 nm with a groove depth of 150 nm and width of 20 μm. However, there are no reports attempting to cut narrow grooves with width of only a few microns. Also, the effect of fs laser pulse duration on the ablation of ITO thin films has not been studied.

In this paper, the roles of laser pulse duration, laser fluence and laser scanning speed are investigated in fs laser patterning of

* Corresponding author. Tel.: +1 785 320 9216; fax: +1 785 532 3738.

E-mail address: bian@ksu.edu (Q. Bian).

ITO thin films in the regime of narrow grooves of a few microns wide. The potential improvement that such high quality narrow grooves could bring in the electrical conversion efficiency is estimated.

2. Experimental procedure

Fig. 1 shows the experimental setup schematically. A fs laser system is used in this study, which consists of a commercially available Ti:sapphire chirped pulse amplifier (CPA) that operates at 1 kHz, seeded by a Rainbow oscillator. The laser beam delivered from this system has center wavelength of 800 nm, repetition rate of 1 kHz, and maximum pulse energy of 5 mJ [19]. The pulse duration is ~ 60 fs right after the amplifier measured by the auto-correlator and can be adjusted by varying the gratings distance of the compressor. A neutral density filter is applied to adjust the pulse energy. The pulse energy is measured with a power meter.

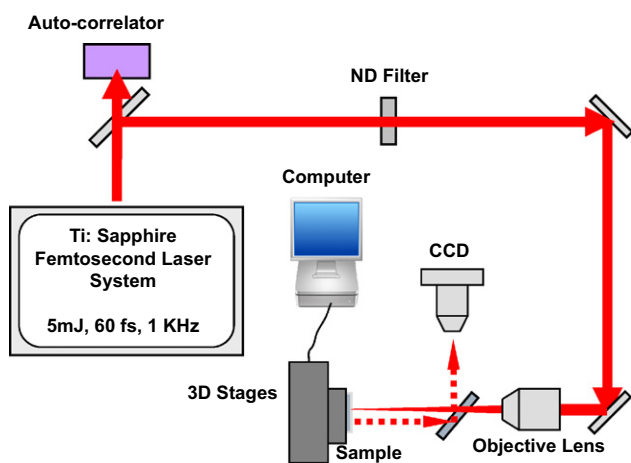


Fig. 1. Schematic of experimental setup.

The laser beam is focused by a lens of 150 mm focal length for single shot damage threshold investigation. An objective lens with 0.3 NA is used for laser grooving experiments. The laser beam is focused on the sample surface. The sample is fixed on a micro-positioning stage controlled by a computer to move in the x , y and z directions.

Commercially available ITO coated glass (Delta Technologies, Ltd.) with sheet resistance of 5–15 Ω is used in the experiments. The soda lime float glass is coated with a primary smoothing layer of SiO_2 , and the layer of indium-tin oxide is vacuum-deposited on it. The thickness of the ITO layer is 120–160 nm.

In this study, the following laser ablation experiments are conducted: (1) to find the material damage threshold and single shot ablation rate at different pulse durations; and (2) to scribe the ITO thin film and investigate how the operating parameters such as pulse duration, pulse fluence and scanning speed affect the groove geometry and surface morphology. Grooves are cut in ITO samples under various conditions, namely variable pulse duration, pulse fluence and laser scanning speed.

To analyze the morphology of the grooves, a KLA Tencor P-16 Profiler and scanning electron microscope (SEM) are used to allow visual comparison in terms of quality and structure in both 2D and 3D. The groove electrical insulation is examined by a multimeter.

3. Results and discussion

3.1. Single pulse ablation morphology and material damage threshold

In order to determine the damage threshold of ITO, we investigated and observed the morphology and depth of crater under single fs laser shot. A typical profile image and two-dimensional cross-section profile of a crater made at fluence of 2 J/cm^2 with 150 mm focal length lens and 60 fs pulse duration are shown in Fig. 2a and b, respectively. From the profile image,

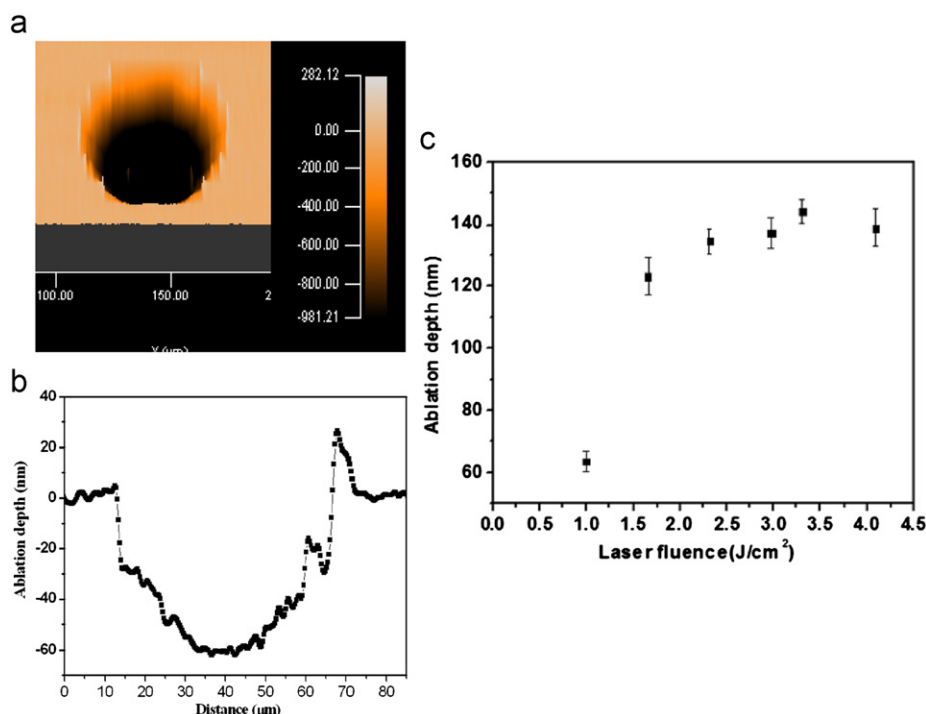


Fig. 2. (a) Profile image of a crater, (b) cross-section profile of the crater, and (c) the ablation depth as a function of laser fluence based on single-shot experiments.

we can observe the crater ablated by the Gaussian beam, and the round shape of the crater confirms the good beam quality. The depth of the crater is around 60 nm and the diameter is about 65 μm at the fluence of 2 J/cm². Fig. 2c shows the ablation depth at 60 fs pulse duration as a function of laser fluence based on single-shot experiments. The crater diameter and depth increase as the laser fluence increases. The nonlinear dependence of ablation depth with fluence is attributed to more efficient multi-photon ionization at higher peak intensities and plasma density increases with the laser intensity rising [20]. Although the 800-nm single photons cannot meet ITO band gap energy requirements, the multiphoton absorption associated with the high intensity of fs pulse is responsible for bond breaking and subsequent emission of electrons and ions.

We studied the single pulse damage threshold of the ITO film by measuring the laser pulse energy which resulted in visible damage to the ITO film. Damage threshold is a characteristic dependent on the wavelength, pulse width and type of material. It is ideally defined as the laser fluence at which irreversible damage occurs in the material by removing a monolayer of material. It is actually determined by visual examination, ablation depth measurement, plasma radiation monitoring, etc. In this study the damage threshold was estimated by recording the diameter (D) and the depth of single-shot ablated craters using SEM and the KLA Tencor P-16 Profiler and then using the following linear relationship between the square of the crater diameter and the logarithm of the laser pulse energy with the Gaussian profile laser beam [21]:

$$D^2 = 2w_0^2 \ln\left(\frac{F_0}{F_{th}}\right) \quad (1)$$

where F_{th} is the damage threshold, F_0 the applied laser fluence and $2w_0$ the Gaussian beam spot size. A plot of the square of damage diameter, D^2 , against the logarithm of energy is made to obtain both the spot size (slope of line) and damage threshold (the extrapolation of D^2 to zero value; Fig. 3a). The damage threshold at 60 fs is found to be 0.21 J/cm². The variations of the damage threshold with pulse duration are shown in Fig. 3b. The damage threshold slightly increases with pulse duration in the sub-ps range, which agrees with the previous research on fs laser ablation of Cu and Al films and fs laser ablation of fused silica [22,23]. It does not totally agree with the observation that the threshold fluence is independent of pulse duration based on the non-equilibrium mechanism of femtosecond laser ablation [20]. Any form of laser energy deposition related to nonlinear effects such as multi-photon ionization is more efficient at high peak intensities as a result of short pulse duration [18].

3.2. The influence of laser fluence on groove morphologies

The laser ablation conditions such as pulse energy and scanning speed should be well controlled in order to achieve required groove dimensions and quality on the ITO thin film. In particular, the major processing parameter is laser fluence. The substrate can be damaged if the laser fluence is too high, while partial removal of ITO film may happen when the fluence is too low.

Fig. 4a shows a 3D groove morphology and Fig. 4b shows the cross-section profiles for different pulse energies. The laser beam was focused by a 30 \times microscope lens. From Fig. 4b, we can observe that for the pulse energy from 125 to 310 nJ the groove depth ranges from 140 to 200 nm, the groove width varies from

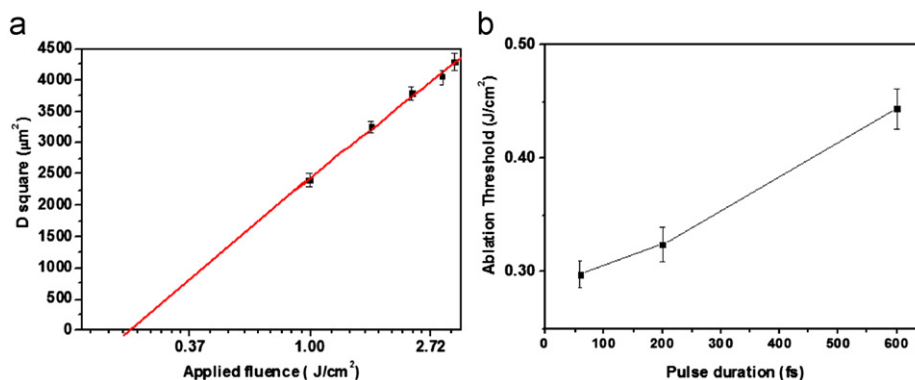


Fig. 3. (a) Material damage threshold at 60 fs and (b) material damage threshold varying with pulse duration.

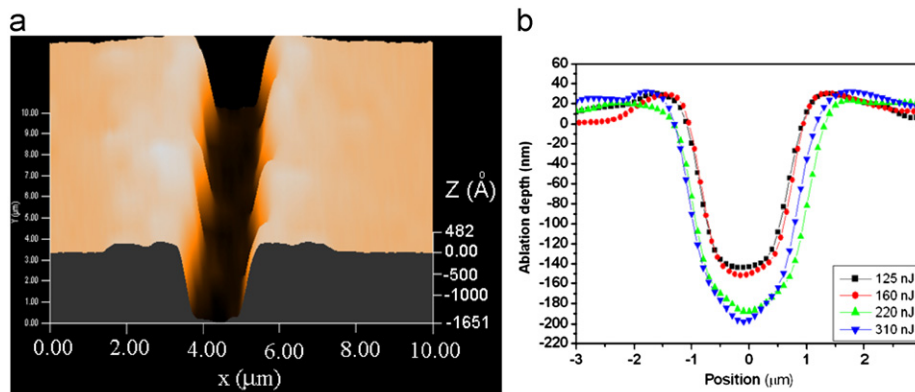


Fig. 4. (a) A typical 3D profile of a groove ablated at the following conditions: pulse energy=160 nJ, scanning speed=0.4 mm/s, and pulse duration=60 fs, (b) 2D cross-section profiles of groove depth with laser energy from 125 to 310 nJ at a scanning speed of 0.4 mm/s.

2 to 3 μm and the ridge height on the edges lies in the range 10–30 nm. With increasing pulse energy, the depth and width of grooves increase, as shown in Fig. 4b. The total amount of energy absorbed by the material increases with increasing pulse energy. The higher laser fluence intensifies the material removal process.

There are ridges on both sides of the grooves. Although heat affected zones have been found to be very small for fs laser pulses in comparison to nanosecond laser pulses in the low fluence regime [24], at high fluences (five times of damage threshold) thermal effects even occur in the femtosecond range and the groove ridges are the results of the thermal effect, which are formed by extruding the melted material by vapor pressure and also by spallation of the thin film layer from the substrate [20].

3.3. The influence of pulse duration on groove morphologies

The dependence of groove quality on pulse duration is also investigated. It is found that detailed structures of the ablated grooves depend strongly on the pulse duration. From the SEM images (Fig. 5a and b) and the 2D cross-section profiles, we find that the groove width decreases from 2.2 to 1.2 μm when tuning the pulse duration from 60 to 600 fs. Furthermore, the groove

depth decreases from 130 to 80 nm when changing the pulse duration from 60 to 600 fs. When the pulse duration increases, the laser intensity decreases and both the groove width and depth decrease at the same fluence.

The formation of these groove ridges is attributed to a surface tension gradient in the molten material near the rim of the laser-irradiated spot, which might have resulted from the poor thermal conductivity of the glass substrate. For fs laser pulses, thermal ablation process also occurs when laser ablation falls in the strong ablation regime with high laser fluence [18,22]. The fs ablation of the ITO thin film in the high fluence mainly governed by thermal process should result in the formation of the ridges because of the high surface temperature of the thin film followed by laser irradiation. Some groove ridges with a height of 5–30 nm were formed at the groove rim as shown in Fig. 5.

There also is a change in groove ridge height from 5 to 30 nm when the pulse duration varies from 600 to 60 fs. The threshold fluence at 60 fs is lower than that at 600 fs; therefore, at the same fluence level, the shorter the pulse duration, the less amount of energy deposited into the processed sample required to remove the same amount of material. As a result, for laser pulse duration within the fs range, the groove ridge height, groove depth and groove width all increase with decreasing pulse duration at the

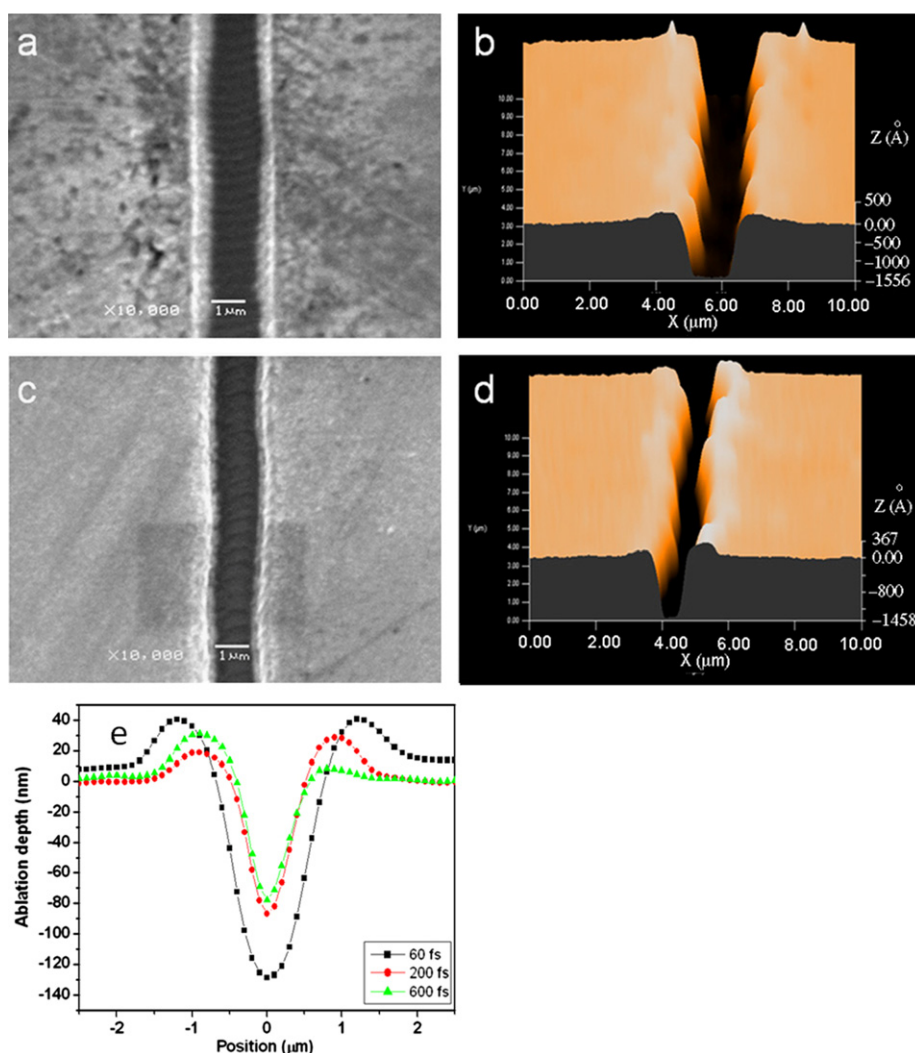


Fig. 5. (a) SEM image of a groove at a pulse energy of 125 nJ, scanning speed of 0.4 mm/s, and pulse duration of 60 fs; (b) 3D profile of the corresponding groove; (c) SEM image of a groove at a longer pulse duration of 600 fs; (d) 3D profile of the corresponding groove; and (e) 2D cross-section of the ablated grooves with pulse durations of 60, 200 and 600 fs.

same fluence level. Thus less pulse is required for the same groove width and depth with the pulse duration decreasing.

3.4. The influence of laser scanning speed on groove morphologies and microstructure

Laser scanning speed affects the groove morphologies and structure at the same energy density since the speed is related to the number of pulses absorbed by the material based on the equation $N=RS/V$, where N is the pulse number, R the pulse repetition rate, S the beam focal spot size and V the laser scanning speed [25].

With fixed pulse energy, repetition rate and focal spot size, the scanning speed is the only parameter that can be varied in order to control the ablation depth. Ablation depth and width at various scanning speeds are shown in Figs. 6 and 7. At a low speed (0.4 mm/s), we can observe the groove with width of 3 μm . At a higher speed (1.2 mm/s), the width decreases to 2 μm . In particular, at the speed of 2 mm/s, the ITO along the groove is only partially removed. Furthermore, with the speed decreasing at

laser fluence well above the damage threshold, the groove depth increases as shown in Fig. 7a, b, c, d, and e. In comparison with the groove at a high speed, the groove at a lower speed is wider and deeper due to the accumulation of the laser irradiation energy. The increase of the ablated depth with decreasing scanning speed is the result of more beam overlap at lower speeds, causing more laser energy accumulation and deposition in the same spot in the ITO thin film [17]. Therefore, we can tune the scanning speed to control the groove depth within the ITO thickness.

3.5. Elemental distribution and electrical resistance across a groove

The grooves are further investigated using the X-ray energy dispersive spectrometer because visual contrast does not reveal the chemical compositions. Fig. 8a shows the SEM image of an ablated groove with the width of 2.5 μm . The point-focused EDS profile from the surface of ITO shows intense In and Sn peaks with O from thin film and glass substrate and Si from glass substrate (Fig. 8b). The line-scanning EDS profiles (Fig. 8c) for In, Sn, O, and Si clearly show a dramatic decrease in the content of In and Sn and a corresponding increase in O and Si along the scanning path from ITO surface to the groove, indicating that the top ITO layer is evaporated and removed, and the glass substrate is exposed.

The electrical resistance is measured to examine the groove quality in terms of electrical insulation. If the groove is not clean or with high ridges (comparable to the thickness of the absorber layer), local shunts and shortcuts may happen through the upper layers of the thin film solar cell, which can reduce the cell conversion efficiency. The groove is not totally electrically insulated as long as the In and Sn are left in the grooves such as shown in Fig. 7d and we can measure the electrical resistance a few hundred ohm. For the insulated grooves as shown in Fig. 7a, b, and c, the measured electrical resistance is infinity (out of the measurement range).

3.6. An example of high quality narrow grooves

By tuning the laser energy to 220 nJ and scanning speed to 1.2 mm/s, the high quality groove as shown in Fig. 9 is achieved. The groove width is 2 μm , the ridge height is small, and the ITO layer is totally removed with negligible damage to the glass substrate as shown in Fig. 9b and c. The elemental analysis in Fig. 9d confirms that there are virtually no ITO residues left in the

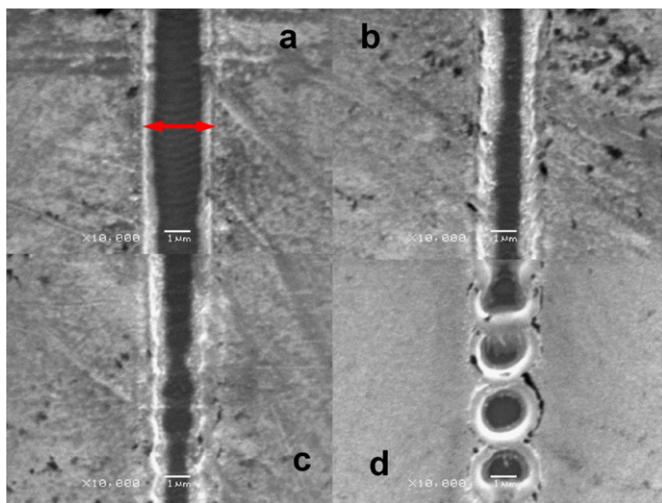


Fig. 6. SEM images of the grooves ablated at a pulse duration of 60 fs, pulse energy of 160 nJ, and scanning speed of 0.4 mm/s (a), 0.8 mm/s (b), 1.2 mm/s (c), and 2 mm/s (d), respectively.

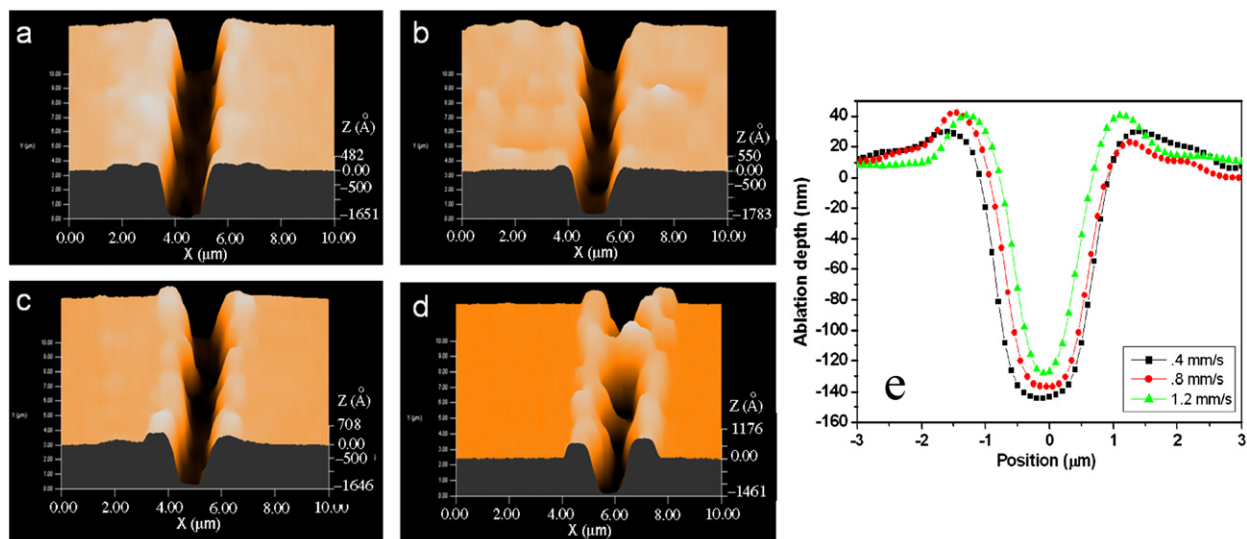


Fig. 7. 3D profile images of the grooves ablated at a pulse duration of 60 fs, pulse energy of 160 nJ, and scanning speed of 0.4 mm/s (a), 0.8 mm/s (b), 1.2 mm/s (c), and 2 mm/s (d), respectively; and (e) groove cross-section profiles at various scanning speeds.

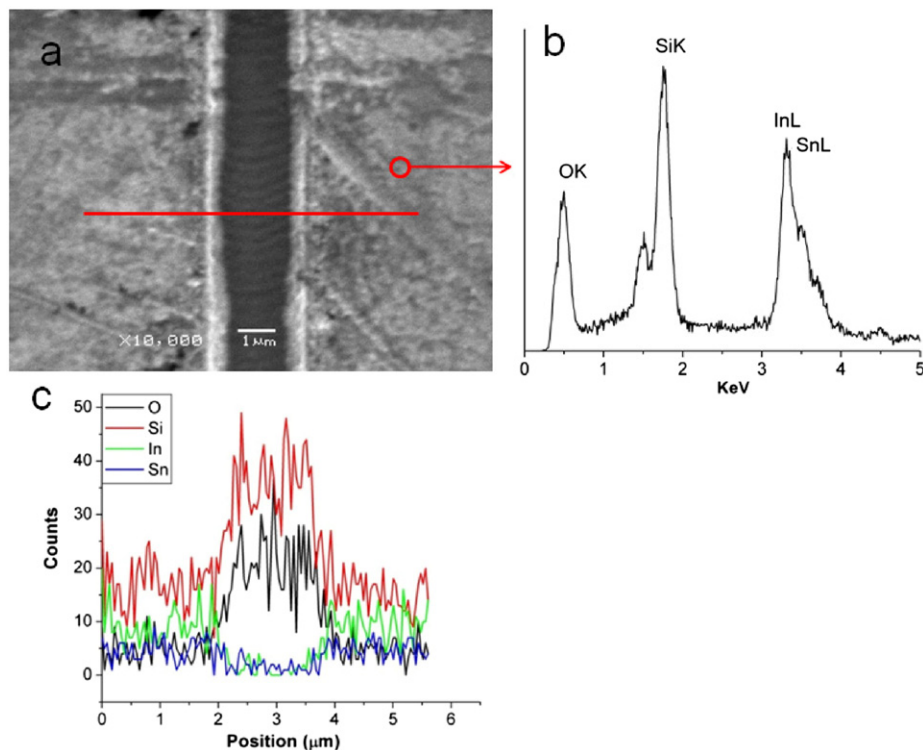


Fig. 8. (a) SEM image of a typical groove ablated at a pulse energy of 160 nJ, scanning speed of 0.4 mm/s, and pulse duration of 60 fs; (b) a point-focused energy-dispersive X-ray spectroscopy (EDS) profile on ITO surface; and (c) EDS line-scanning profile of a groove ablated in the ITO layer to expose the substrate.

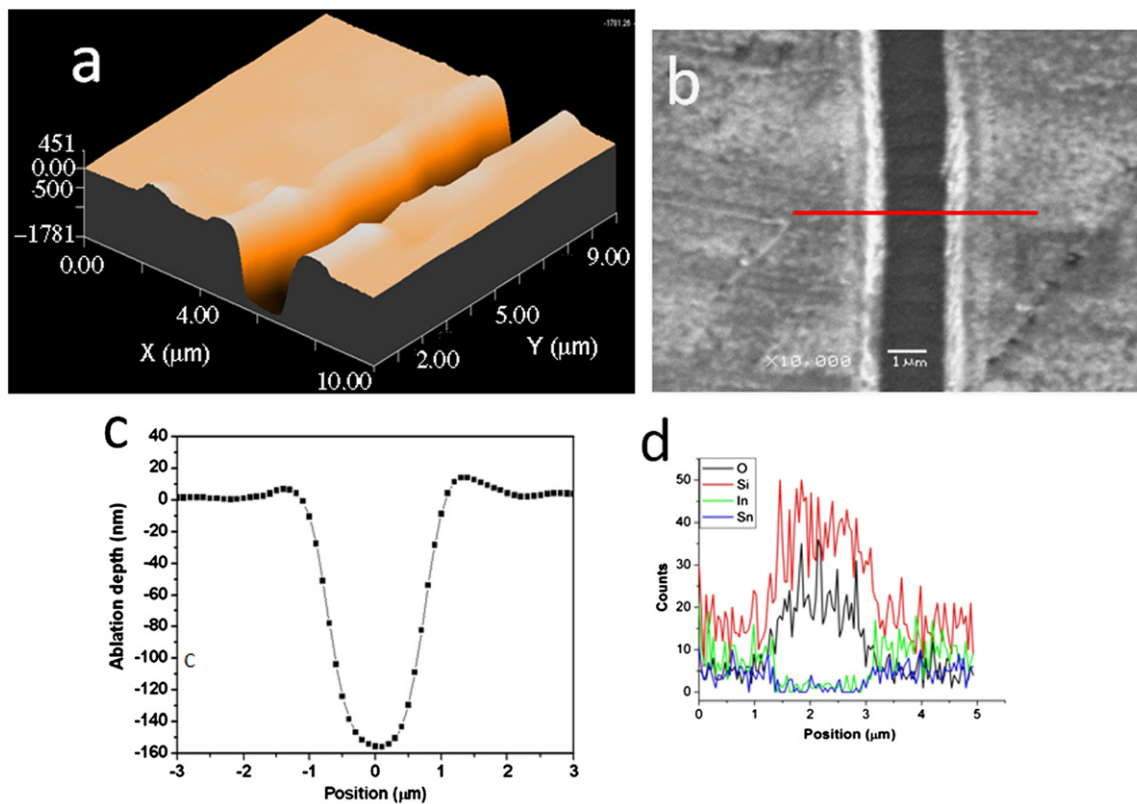


Fig. 9. (a) 3D image of a high quality groove ablated at a pulse energy of 220 nJ, scanning speed of 1.2 mm/s, and pulse duration of 60 fs; (b) SEM image of the groove; (c) 2D cross-section of the groove, and (d) EDS line-scanning profile of the groove.

groove. The electrical resistance is examined using the multi-meter and the result indicates that the groove is electrically insulated. High quality narrow grooves like the one shown in

Fig. 9 could significantly increase the electrical conversion efficiency of thin film solar cells. For illustration purposes, if all three interconnection grooves can be made to a few microns in width

using the commonly known three patterning processes (e.g. P1, P2 and P3) in the monolithic solar modules, the dead area of the thin film solar cell can be decreased from 75–150 μm to 30–60 μm , which means that the cell active area will increase by 0.75–1.5% if the cell width is 6 mm [2].

Therefore, high quality narrow grooves are highly desirable in manufacturing thin film solar cells, and femtosecond laser is a promising tool for producing these grooves.

4. Conclusions

In summary, the femtosecond laser with various energy, pulse durations, and scanning speeds has been utilized to pattern ITO glass for thin film solar cells. The damage threshold of the ITO thin film is found to be 0.21–0.40 J/cm^2 when the pulse duration varies from 60 to 600 fs. The single pulse ablation rate increases with increasing laser fluence and decreasing pulse duration and scanning speed due to the accumulation of the laser irradiation energy. In addition, the groove width is insignificantly affected by pulse duration. The groove width decreases with increasing pulse duration. Also, we need to control the scanning speed to fully remove ITO without damaging the glass. We can tune the processing parameters to fabricate the required structure. For example, grooves without damaging the substrate can be made at the optimized parametric regime: the laser fluence is 2.2–5 J/cm^2 and the scanning speed is 0.4–1.2 mm/s for a 1 kHz laser. With the selective laser energy and laser scanning speed, a high quality groove about 2 μm wide, 150 nm deep and 10 nm in ridge height is obtained, which shows the potential of fs laser for producing high density interconnects in thin film solar cells and thus significantly increasing the solar cell conversion efficiency.

Acknowledgments

Financial support of this work by the DoD Army Research Office under the Agreement no. W911NF-07-1-0475 and partial support by the National Science Foundation under Grant no. CMMI-1131627 is gratefully acknowledged.

References

- [1] Chopra KL, Paulson PD, Dutta V. Thin-film solar cells: an overview. *Progress in Photovoltaics* 2004;12(2–3):69–92.
- [2] Rowell MW, McGehee MD. Transparent electrode requirements for thin film solar cell modules. *Energy and Environmental Science* 2010;4(1):131–4.
- [3] Kessler F, Herrmann D, Powalla M. Approaches to flexible CIGS thin-film solar cells. *Thin Solid Films* 2005;480:491–8.
- [4] Wiedeman S, Wendt RG, Britt JS. Module interconnects on flexible substrates. 1999. USA: AIP; 1999 p. 17–22.
- [5] Aberle AG. Thin-film solar cells. *Thin Solid Films* 2009;517(17):4706–10.
- [6] Hoheisel M, Mitwalsky A, Mrotzek C. Microstructure and etching properties of sputtered indium-tin oxide (ITO). *Physica Status Solidi (a)* 1991;123(2):461–72.
- [7] Lee S, Yang DF, Nikumb S. Femtosecond laser patterning of Ta0.1W0.9Ox/ITO thin film stack. *Applied Surface Science* 2007;253(10):4740–7.
- [8] Henry M, Harrison PM, Wendland J. Laser direct write of active thin-films on glass for industrial flat panel display manufacture. *Journal of Laser Micro Nanoengineering* 2007;2(1):49–56.
- [9] Kim J, Na S. Metal thin film ablation with femtosecond pulsed laser. *Optics and Laser Technology* 2007;39(7):1443–8.
- [10] Yang JJ, Wang R, Liu W, Sun Y, Zhu XN. Investigation of microstructuring CuInGaSe₂ thin films with ultrashort laser pulses. *Journal of Physics D—Applied Physics* 2009;42:21.
- [11] Raciukaitis G. Laser structuring of conducting films on transparent substrates for electronics devices. Riga, Latvia: SPIE; 2008. Optical Society of America (OSA); European Optical Society (EOS); University of Latvia; Latvian Council of Science; 2008.
- [12] Bovatsek J, Tamhankar A, Patel RS, Bulgakova NM, Bonse J. Thin film removal mechanisms in ns-laser processing of photovoltaic materials. *Thin Solid Films* 2009;518(10):2897–904.
- [13] Dubey AK, Yadava V. Laser beam machining—a review. *International Journal of Machine Tools and Manufacture* 2008;48(6):609–28.
- [14] Raciukaitis G, Gecys P, Trusovas R, Kondrotas R. Picosecond laser scribing for thin-film solar cell manufacturing. Wuhan, China: Laser Institute of America; 2010.
- [15] Molpeceres C, Lauzurica S, Ocana J, Gandia J, Urbina L, Carabe J. Microprocessing of ITO and a-Si thin films using ns laser sources. *Journal of Micro-mechanics and Microengineering* 2005;15(6):1271–8.
- [16] Choi HW, Farson DF, Bovatsek J, Arai A, Ashkenasi D. Direct-write patterning of indium-tin-oxide film by high pulse repetition frequency femtosecond laser ablation. *Applied Optics* 2007;46(23):5792–9.
- [17] Park M, Chon BH, Kim HS, Jeoung SC, Kim D, Lee JI, et al. Ultrafast laser ablation of indium tin oxide thin films for organic light-emitting diode application. *Optics and Lasers in Engineering* 2006;44(2):138–46.
- [18] Ashkenasi D, Muller G, Rosenfeld A, Stoian R, Hertel IV, Bulgakova NM, et al. Fundamentals and advantages of ultrafast micro-structuring of transparent materials. *Applied Physics A: Materials Science and Processing* 2003;77(2):223–8.
- [19] Chen S, Chini M, Wang H, Yun C, Mashiko H, Wu Y, et al. Carrier-envelope phase stabilization and control of 1 kHz, 6 mJ, 30 fs laser pulses from a Ti:sapphire regenerative amplifier. *Applied Optics* 2009;48(30):5692–5.
- [20] Gamaly EG, Rode AV, Luther-Davies B, Tikhonchuk VT. Ablation of solids by femtosecond lasers: ablation mechanism and ablation thresholds for metals and dielectrics. *Physics of Plasmas* 2002;9(3):949–57.
- [21] Liu JM. Simple technique for measurements of pulsed Gaussian-beam spot sizes. *Optics Letters* 1982;7(5):196–8.
- [22] Le Harzic R, Breiting D, Weikert M, Sommer S, Fohl C, Valette S, et al. Pulse width and energy influence on laser micromachining of metals in a range of 100 fs to 5 ps. *Applied Surface Science* 2005;249(1–4):322–31.
- [23] Perry MD, Stuart BC, Banks PS, Feit MD, Yanovsky V, Rubenchik AM. Ultrashort-pulse laser machining of dielectric materials. *Journal of Applied Physics* 1999;85(9):6803–10.
- [24] Le HR, Huot N, Audouard E, Jonin C, Laporte P, Valette S, et al. Comparison of heat-affected zones due to nanosecond and femtosecond laser pulses using transmission electronic microscopy. *Applied Physics Letters* 2002;80(21):3886.
- [25] Wang ZB, Hong MH, Lu YF, Wu DJ, Lan B, Chong TC. Femtosecond laser ablation of polytetrafluoroethylene (Teflon) in ambient air. *Journal of Applied Physics* 2003;93(10):6375–80.